DIFFUSION AND/OR PLASTIC DEFORMATION AROUND FLUID INCLUSIONS IN SYNTHETIC QUARTZ: NEW INVESTIGATIONS.

Anne-Marie BOULLIER (*), Gérard MICHOT (&), Arnaud PECHER (*/$) and Odile BARRES (#).

* Centre de Recherches Pétrographiques et Géochimiques, B.P.20, 54501 VANDOEUVRE LES NANCY CEDEX, FRANCE.
& Laboratoire de Physique du Solide, Ecole Nationale Supérieure des Mines et de la Métallurgie, Parc de Saurupt, 54000 NANCY, FRANCE.
$ Laboratoire de Géologie structurale, Ecole Nationale Supérieure des Mines et de la Métallurgie, Parc de Saurupt, 54000 NANCY, FRANCE.
# Laboratoire de Spectrométrie de Vibrations, Université de Nancy I, B.P.239, 54506 VANDOEUVRE LES NANCY CEDEX, FRANCE.

ABSTRACT. Synthetic quartz containing fluid inclusions (H_2O + NaOH, 0.5N) was annealed at high temperature (T=448°C) and under confining pressure (P_c=200 or 350MPa). Changes in the shape of the inclusions were observed together with variations of their filling densities which depend on the value of the internal pressure, P_i; the latter tends to equilibrate with the confining pressure P_c either by decrepitation or by progressive evolution. X-ray topography after treatment reveals contrast around the modified fluid inclusions. T.E.M. investigations show some dislocations around the inclusions after experiment. However, IR microspectroscopy does not show any visible change in the water absorption band in samples before and after annealing.

These results are discussed and some interpretations are proposed. As demonstrated by previous authors (Gratier and Jenatton, 1984) the changes in the shape are due to solution - deposition processes. Plastic deformation around fluid inclusions is probably largely responsible for the changes in density, but diffusion processes (positive and negative exchanges between quartz and fluid inclusion) cannot be entirely excluded. The driving force may be the elastic strain energy due to the difference in pressure between the fluid inclusion and the confining medium (Doukhan and Trépied, 1985).

1. INTRODUCTION.

Recent experimental work has shown that fluid inclusions in synthetic quartz underwent strong shape and density modifications when submitted to P-T conditions which are different from those on their trapping isochore line and where the internal pressure is larger than the confining pressure (Sabouraud, 1981; Pêcher, 1981; Gratier and Jenatton, 1984; Pêcher and Boullier, 1984). Complementary experiments have been performed on the same material for the case where the internal pressure is lower than the confining pressure.

D. Bridgwater (ed.), Fluid Movements – Element Transport and the Composition of the Deep Crust, 345–360.

This work presents the results of these experiments and of some investigations with X-ray topography, transmission electron microscopy and infrared microspectroscopy.

2. THE EXPERIMENTS.

2.1. Starting material.

Synthetic quartz crystal (S.I.C.N., Annecy, France), grown hydrothermally in a 0.5N NaOH solution following the Régrény's method (1973) was used. The seed contains numerous large cylindrical fluid inclusions which are orientated in a direction near the c axis of the crystal (figure 1). X-Ray topographs before experiments (figure 2) reveal that the fluid inclusions are localized on straight dislocations (Wilkins and McLaren, 1981; Michot et al., 1984); consequently, these fluid inclusions probably originated by corrosion of the cores of the dislocation before saturation conditions were attained in the autoclave. When saturation is reached (160MPa, 365°C), quartz growth blocks the tubes which are filled with a fluid with a density equal to that within the autoclave (0.8).

2.2. The initial homogenization temperatures.

The samples (0.8x2.5x5mm) are cut and two faces polished which contain a and c. Homogenization temperatures (Th) are measured before the experiments with a Chaix-Meca stage (Poty et al., 1976). They are very homogeneous in each sample (figure 3) but vary slightly from sample to sample (for instance 244.6°C for 2A10 and 247.6°C for 2A6). Controls by calibrations have shown that these differences are not due to measurements errors.

Only few P-V-T data are available on the system H_2O + NaOH + SiO_2. Régrény (1973) has shown that the isochores are subparallel to isochores in the pure H_2O system, but slightly shifted towards higher temperatures. Consequently, we will use the slopes of the isochores given by Burnham et al. (1969) for pure H_2O which are very close to the P-V-T data of Zang and Frantz (1987).

2.3. Principle and conditions of the experiments.

Fluid inclusions can be considered as micro-autoclaves in which the internal pressure (P_i) is a function of the temperature and molar volume of the fluid (figure 4). The confining pressure (P_c) is an external thermodynamic parameter of the system but it also prevents decrepitation of the fluid inclusions. Only one type of experiment has been performed so far; it corresponds to P_i higher than P_c (argon) (Pêcher and Boullier, 1984):

P_c(argon) = 200 MPa, T = 448°C (Figure 4)

These experiments have now been supplemented by experiments with a confining pressure P_c lower than P_i:

P_c(argon) = 350 MPa, T = 448°C.

To test the influence of a chemical gradient of water between the inclusion and the confining medium, experiments have been performed with water (rather than argon) as a fluid medium generating the confining pressure P_c (either higher or lower than P_i):

P_c(water) = 200 or 350 Mpa, T = 448°C.

All the experiments are reported in table 1.

3. EXPERIMENTAL RESULTS.

3.1. P_c(argon) lower than P_i.

A comparison of samples before and after the experiments shows important modifications of the shape and the density of the fluid inclusions (see Pêcher and Boullier, 1984). We distinguish two different behaviours: 1) the inclusions decrepitate as demonstrated by microfracturation or 2) the fluid inclusions do not decrepitate, but their shape and density are modified.

3.1.1. Changes of shape. They have already been described in detail for such experiments by Pêcher and Boullier (1984); in this paper, we will only refer to the most striking features.

a - decrepitated inclusions: microfractures contain numerous small fluid inclusions (secondary fluid inclusions or "decrepitation cluster", Swanenberg, 1980), the size of which decreases towards the external limit of the crack (20 to 2 μm); they have homogeneous filling ratios. They appear during decrepitation and then are healed by growth of quartz from the fracture walls (Lemmlein and Kliya, 1954; Smith and Brians, 1984).

b - undecrepitated fluid inclusions: the most striking feature of the undecrepitated fluid inclusions is a decrease of their length/width ratio towards an equilibrium value (2.7, figure 5), together with the appearance of rational walls (simple pyramidal and prismatic crystalline faces). Their evolution with time depends on the orientation of the initial fluid inclusion relative to the c axis of the quartz crystal. Generally, they tend towards the shape of a negative crystal shape (for details see Pêcher and Boullier, 1984).

3.1.2. Changes of homogenization temperatures. The temperatures of homogenization measured after experiments are reported in figure 6. The Th measurements are grouped into two sets for each sample: 1- the first one with slightly scattered but high values (up to 280°C) corresponds to decrepitated primary inclusions or secondary inclusions formed by decrepitation of the former ones. 2- the second set with values slightly higher than the initial Th, corresponds to the undecrepitated primary inclusions. The difference in the homogenization temperature increases with the duration of the experiment (figure 7): for the longest experiment (2A6), the difference is 13°C corresponding to a density decrease of 0.019.

3.2. P_c(argon) higher than P_i.

As for the above experiments, important changes of shape and density of the fluid inclusions are observed after annealing.

3.2.1. Changes of shape. In the case where the confining pressure P_c(argon) is greater than the internal pressure P_i, the changes of shape are somewhat similar to those observed in the previous case ($P_c<P_i$) except that the equilibrium shape ratio is lower (1.8, ;figure 5) and corresponds to a bipyramid without a prism.

3.2.2. Changes of homogenization temperatures. Figure 8 shows histograms of the homogenization temperature after experiment in the case where P_c is higher than P_i. Th is clearly shifted towards lower values (increase of the density), but the values are much more scattered than for the previous experiments and there is no well defined maximum. However, it should be noticed that the larger the inclusion volume, the bigger the difference between initial Th and final Th (figure 9).

3.3. Experiments with water as a confining medium.

Two experiments have been performed to test the influence of a possible chemical gradient of water between the inclusion and the confining medium. A sample was placed in a gold capsule containing water; the capsule was sealed and placed in the autoclave where the pressure medium is argon. Considering the solubility of quartz in water in the experimental conditions, the samples were polished again after the experiment for observations and for Th measurements. No damage is caused by that polishing.

These experiments do not show any difference to the previous ones (with argon as confining medium). The changes of shape and density are fully comparable to those observed for corresponding experiments (P_c lower or higher than P_i). Consequently, experimental results are given on the same figures (figures 5 to 8).

4. X-RAY TOPOGRAPHS.

4.1. Before experiment.

On X-ray topographs (Lang chamber), the samples show long straight dislocations as observed by Wilkins and McLaren (1981) in comparable synthetic quartz crystals. Fluid inclusions are not visible on X-ray topographs recorded at room temperature (figure 2). However, one series of topographs was obtained with the LURE synchrotron (Orsay, France), the sample being heated to 302°C (Michot et al., 1984). As soon as Th is reached, contrast appears around fluid inclusions which becomes visible in this way. If the temperature decreases below Th, the contrast around the fluid inclusions disappears except around some of those which have decrepitated. Consequently, in the experiments of Michot et al. (1984), the contrast around fluid inclusions is related to elastic deformation of the quartz crystals, due to an increase of pressure in the fluid inclusion.

4.2. After experiments.

X-ray topographs were performed on some samples after experiments. In every case, a permanent contrast is observed around fluid inclusions at room temperature, for experiments at P_c either lower or higher than P_i (figure 10). The contrast around fluid inclusions is very strong. If it is due to dislocations, then their density is higher than $10^5 cm^{-2}$. The shape of the contrast seems to be intermediate between the initial and the final shape of the fluid inclusions. This would indicate that the contrast is due to a mechanism which operates during the whole experiment and is not due to the final stage of the experiment (decrease of T and P_c).

5. PRELIMINARY TEM OBSERVATIONS.

After experiment, standard polished thin section (30µm thick) were made which were then thinned to less than 1µm using an ion thinner. As the probability of obtaining a thin area exactly around a fluid inclusion is very small, only one ion thinning was successful. The sample was studied with a JEOL 200CX transmission electron microscope at the Service Commun d'Analyses of the Nancy I University. Dislocations are observed at the tip of the fluid inclusion (sample 2A4, figure 11); they are roughly parallel to the c axis but their Burgers vector has not been characterized. Their density is approximately 10^7 cm^{-2}. Some very small defects are also observed but their exact nature has not been identified; they

could be very small bubbles, such as those observed by Kirby and McCormick (1979) in experimentally deformed synthetic quartz crystals and by McLaren et al. (1983) in heated synthetic quartz crystals, due to precipitation of water above the equilibrium concentration (Doukhan and Paterson, 1986; Cordier et al., in press).

6. INFRARED MICROSPECTROSCOPY DATA.

Infrared spectra were recorded with a Brucker IFS 88 Fourier transform spectrometer which is provided with a microscope. The samples investigated were unmodified and modified (before and after experiments), double polished and 800 μm thick. Two types of spectra were obtained for the specific seed under study for wavenumbers between 3600 and 3000cm^{-1}.This region corresponds to water or OH absorption bands in quartz (Kats, 1962; Aines and Rossman, 1984; Kronenberg et al., 1984). Flat spectra were observed for the major part of the seed, and spectra with high absorption for a region close to numerous and unusually large fluid inclusions. These discrepancies could be related to defects pre-existing in the seed before the hydrothermal growth of the synthetic quartz.

However, in the same area, spectra are identical before and after the experiment, even if performed very close to a fluid inclusion (figure 12). Consequently, it seems that any modification of the water distribution is too small to be detected with such a method.

7. DISCUSSION.

7.1. Changes of shape.

It is characterized by a decrease of the shape ratio (l/w) of the fluid inclusions (figure 5). In the case where P_c is lower than P_i (P_c = 200MPa), the decrease of l/w is faster for undecrepitated fluid inclusions where P_i is high (282MPa) than for decrepitated fluid inclusions where P_i is roughly equal to P_c (P_i= 200MPa). This phenomenon was described by Gratier and Jenatton (1984) for experiments realized at atmospheric pressure. These authors demonstrated that the change of shape is due to a solution - deposition process. The variation of the chemical potential at different points of the liquid - solid interface, caused by variation of the surface energy with the curvature, is the driving force and the rate of the l/w decrease is controlled by the rate of dissolution in the median part of elongated inclusions.

In this study (P_i = 282MPa, T = 448°C), the equilibrium shape is reached after only 350h; it corresponds to a configuration with minimum surface energy and depends on the confining pressure.

7.2. Changes of the homogenization temperatures.

7.2.1 Decrepitated inclusions. Decrepitation of fluid inclusions has been experimentally reproduced by Leroy (1979) without confining pressure and by Pêcher (1981) in synthetic quartz and by Sabouraud (1981) in fluorine with a confining pressure. In our experiments, the occurrence in the same sample of decrepitated and undecrepitated fluid inclusions with roughly identical volume and shape indicates that P_i-P_c (P_i>P_c) was near the decrepitation overpressure value; actually, considering the P_c-V-T conditions, the overpressure (82MPa) is similar to the value obtained at atmospheric pressure and 280°C by Leroy (1979) for large fluid inclusions ($V > 2 \times 10^4$ μm^3) in synthetic quartz (85MPa).

We may consider that there is a competition during crack development between the

confining pressure P_c and the internal pressure P_i and that the crack stops when both pressures are almost equal. In this case, the density of secondary inclusions in the healed crack would correspond to the P_c-T conditions. Actually, Th measurements on secondary inclusions (271°C for 2A7, 269°C for 2A1, 272°C for 2A6) indicate pressures of the order of 200 to 220MPa for T = 448°C.

7.2.2. Undecrepitated fluid inclusions. Even for the undecrepitated fluid inclusions, variations of Th are observed which are independent of the changes of shape (compare figures 5 and 7). These variations are either positive ($P_c<P_i$) or negative ($P_c>P_i$) and correspond to reverse variations of density of the fluid in the inclusions. The experiments performed in a water confining medium showed the same density modifications as for the argon experiments. Consequently, we believe that the chemical gradient of water between the inclusion and the confining medium is not the driving force for variation in the density. The driving force could be the volume dependent elastic strain energy due to the difference in pressure between the fluid inclusion and the confining medium (Doukhan and Trépied, 1985).Three possibilities may be envisaged: i) the included fluid diffuses along the long and straight dislocations on which the inclusions are located; ii) there is a variation of the volume of the inclusion due to plastic deformation of surrounding quartz, related to the difference between P_i and P_c; iii) the volume of the inclusion is constant but water diffuses away from or towards the fluid inclusions through the surrounding quartz.

Comparing the two types of experiments, the first hypothesis is rejected because it cannot explain the increase of density where $P_c>P_i$.The occurrence of dislocations around the fluid inclusions indicates that some plastic deformation has occurred, and that the volume of the inclusion varied during the experiments. The observed dislocation density ($\approx 10^7$ cm^{-2}) is compatible with the volume change required to justify such a density variation. If plastic deformation alone is operative, we cannot explain why the density variation is volume independent where $P_i>P_c$ and volume dependent where $P_i<P_c$.

The similar IR spectra obtained on samples before and after the experiments indicate that any diffusion of water is too small to be detected by this method. However, exchange of water between the quartz matrix and the fluid inclusion cannot definitely be excluded, because of the low sensitivity of the IR microspectrometric measurements.

Actually, such a process might explain better some discrepancies between both types of experiments:

-at $P_i>P_c$, Th variations are very homogeneous (volume independant); that would correspond to easy diffusion of H towards the quartz matrix because of its relatively low content in H/Si defects (less than 300ppm, D.Mainprice, comm. pers.).

-at $P_i<P_c$ Th variations are scattered and volume dependent. This would correspond to less easy diffusion of H from the quartz matrix towards the inclusion (long distances due to low content in H/Si defects). Large inclusions have greater elastic energy and are thus more able to attract H ions.

8. CONCLUSIONS.

The experiments described in this paper have shown that important changes of shape and density occur when fluid inclusions are submitted to P_c-T conditions different from their trapping ones. As demonstrated by previous authors (Gratier and Jenatton, 1984), the changes in shape are due to solution - deposition processes. Plastic deformation around fluid inclusions is probably responsible for the changes in density, but diffusion processes (positive and negative exchange between quartz and fluid inclusion) cannot be entirely excluded. More systematic and precise investigations are needed to understand fully the

changes in density of the fluid inclusions. In any case the driving force for deformation or diffusion could be the elastic strain energy due to the difference in pressure between the fluid inclusion and the confining medium (Doukhan and Trépied, 1985).

We have to be cautious when extending our observations to natural fluid inclusions because of the peculiar characteristics of the material used for these experiments (relatively wet synthetic quartz crystal, very long and rectilinear dislocations, NaOH + H_2O filling of the inclusions...). However, these results can explain the often observed discrepancies in natural samples between fluid inclusion data and thermobarometric calculations using mineralogical assemblages, and the difficulty in finding fluid inclusions corresponding to the climax of metamorphism (Coolen, 1982; Pêcher, 1979, 1984; Sauniac and Touret, 1983). However, the observed modifications imply high temperature processes (plastic deformation and perhaps diffusion). Consequently, fluid inclusion studies are still meaningful and useful for the knowledge of the nature of the fluids and the P-T conditions operating during low temperature geological phenomena.

ACKNOWLEDGEMENTS. The authors wish to thank especially J.C.Doukhan for stimulation and constructive remarks and A.George, C.Ramboz, A.Burneau and Y.G.Zang for fruitful discussions. They are also grateful to M.Pichavant and A.Rouillier for help in experimental techniques and to W.L.Brown who kindly improved the english text. This project was supported by the C.N.R.S. (A.T.P. Physique des Hautes Pressions). Contribution C.R.P.G. n°798

REFERENCES.

Aines R.D. and Rossman G. (1984). 'Water in minerals? A peak in the infrared.' J. Geoph. Res., **89**, 4059-4071.

Burnham C.W., Holloway F.R. and Davis N.F. (1969). 'Thermodynamic properties of water to 1000°C and 10000bars'. Geol. Soc. America Sp. paper, **132**, 96p.

Coolen J.J.M.M. (1980). 'Chemical petrology of the Furua granulite complex, southern Tanzania.' G.U.A. papers of geology, Amsterdam, 1, **13**, 258p.

Cordier P., Boulogne B. and Doukhan J.C. (1988). 'Water precipitation and diffusion in wet quartz and wet berlinite $AlPO_4$.' Bulletin de Minéralogie., **111**, 113-137.

Doukhan J.C. and Paterson M.S. (1986). 'Solubility of water in quartz. A revision.' Bull. Minéral., **109**, 193-198.

Doukhan J.C. and Trépied L. (1985). 'Plastic deformation of quartz single crystals.' Bull. Minéral., **108**, 97-123.

Gratier J.P. and Jenatton L. (1984). 'Deformation by solution - deposition and reequilibration of fluid inclusions in crystals depending on temperature, internal pressure and stress.' Journ. Struct. Geol., **5**, 329-339.

Kats A. (1962). 'Hydrogen in alpha-quartz.' Philips Res. Rep., **17**, 1-31, 133-279.

Kirby S.H. and McCormick J.W. (1979). 'Creep of hydrolytically weakened synthetic quartz crystals oriented to promote {2110} <0001> slip: a brief summary of work to date.' Bull. Mineral.,**102,** 124-137.

Kronenberg A.K., Kirby S.H., Aines R.D. and Rossman G.R. (1986). 'Solubility and diffusional uptake of hydrogen in quartz at high water pressures: implications for hydrolytic weakening.' Journ. Geoph. Res., **91**, B12, 12723-12744.

Lemmlein G.C. and Kliya M.O. (1954). 'Changes in fluid inclusions under the effect of temporary heating up of a crystal'. Akad. Nauk. SSSR Doklady, **94,** 233-236 (in russian).

Leroy J. (1979). 'Contribution à l'étalonnage de la pression interne des inclusions fluides lors de leur décrépitation.' Bull. Minéral., **102**, 584-593.

McLaren A.C. A.C., Cook R.F., Hyde S.T. and Tobin R.C. (1983). 'The mechanisms of the formation and growth of water bubbles and associated dislocation loops in synthetic quartz.' Phys. Chem. Minerals, **9**, 79-94.

Michot G., Weil B. and George A. (1984). 'In situ observation by synchrotron X-Ray topography of the evolution with temperature of fluid inclusions in synthetic quartz.' Journal Crystal Growth, **69**, 627-630.

Pêcher A. (1979). 'Les inclusions fluides des quartz d'exsudation de la zone du M.C.T. himalayen du Népal central'. Bull. Minéral.,.**102**, 537-554.

Pêcher A. (1981). 'Experimental decrepitation and reequilibration of fluid inclusions in synthetic quartz.' Tectonophysics, **78** , 567-584.

Pêcher A. (1984). 'Chronologie et rééquilibrage des inclusions fluides: ;quelques limites à leur utilisation en microthermométrie.' Thermométrie et barométrie géologiques, éd. M.Lagache, Soc. Fr. Minéral. et de Cristall., 463-485.

Pêcher A. et Boullier A.M. (1984). 'Evolution à pression et température élevées d'inclusions fluides dans un quartz synthétique.' Bull. Minéral., **107**, 139-153.

Poty B., Leroy J. et Jachimowicz L. (1976). 'Un nouvel appareil pour la mesure des températures sous le microscope: l'installation de microthermométrie Chaix Méca'. Bull. Soc. fr. Minéral. Cristallogr., **99**, 182-186.

Régrény A. (1973). 'Recristallisation hydrothermale du quartz.' Thèse Doct. Ing. Paris VI, 133p.

Sabouraud C. (1981). 'Décrépitation expérimentale d'inclusions sous pression. Application au cas d'inclusions primaires de fluorine.' C. R. Acad. Sc. Paris, **292**, 729-732.

Sauniac S. and Touret J. (1983). 'Petrology and fluid inclusions of a quartz-kyanite segregation in the main thrust zone of the Himalayas.' Lithos, **16** , 35-45.

Smith D.L. and Evans B. (1984). 'Diffusional crack healing in quartz.' J. Geoph. Res., **89**, 4125-4135.

Swanenberg H.E.C. (1980). 'Fluid inclusions in high-grade metamorphic rocks from SW Norway.' Thesis **25**, Rijksuniversiteit Utrecht, 147p.

Wilkins R.W.T. and McLaren A.C. (1981). 'The formation of primary inclusions from etch pits in crystals.' N. Jb. Miner. Mh., **5**, 220-224.I

Zang Y.G. and Frantz J.D. (1987). 'Determination of the homogenization temperatures and densities of supercritical fluids in the system NaCl-KCl-$CaCl_2$-H_2O using synthetic fluid incusions.' Chemical Geology, **64** in press.

TABLE 1 - EXPERIMENTS.

Sample	t	T	Pc	Thi
2A7	69h 15'	448°C	200MPa	246.5°C
2A1	70h 15'	447°C	200MPa	246.5°C
2A9	153h 40'	448°C	200MPa	246.5°C
2A2	162h 35'	447°C	200MPa	246.3°C
2A14a	325h 15'	446°C	200MPa	246.0°C
2A10	351h	448°C	200MPa	244.6°C
2A4	409h	447°C	200MPa	246.3°C
2A3	1220h	448°C	200MPa	246.3°C
2A6	3064h	447°C	200MPa	247.6°C
2A12c	71h	447°C	350MPa	251.8°C
2A11c	192h 3'	447°C	350MPa	251.9°C
2A12b	484h 28'	447°C	350MPa	249.9°C
2A11b	1036h 52'	446°C	350MPa	250.1°C
2A8a	2086h 304	446°C	350MPa	249.7°C (large I.F. 246.5°C (small I.F.)
			$Pc(H_2O)$	
2A13b	288h 40'	447°C	200MPa	246.5°C
2A8c	281h 55'	446°C	350MPa	248.6°C

Table 1. Summary of the experiments with different duration (t) at the temperature T and under confining pressure P_c. Thi is the mean of the initial homogenezation temperature (before experiments).

Figure 1. Microphotograph of a thick section in the synthetic quartz crystal seed. Note the large fluid inclusions which are subparallel to the c axis. Compare with the X-ray topograph before experiment (figure 2).

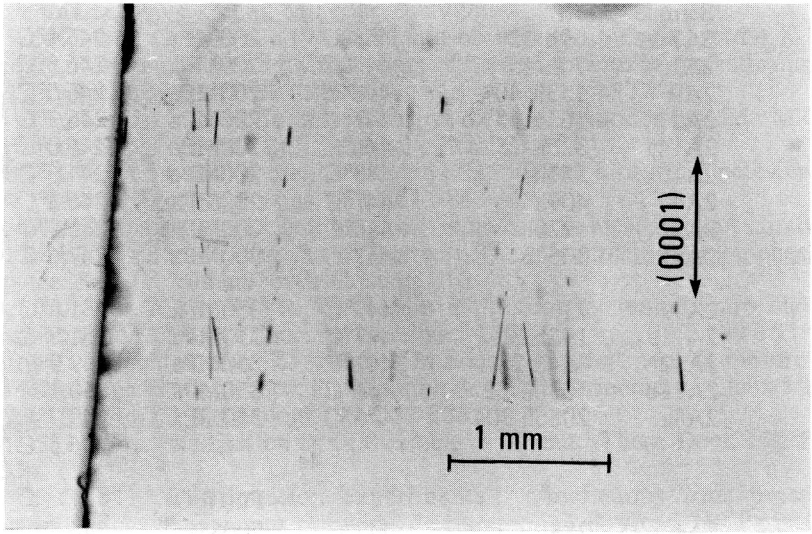

Figure 2. X-ray topograph of the 2A14a sample before experiment. Note the long and straight dislocations subparallel to the c axis and crossing the seed into the hydrothermally grown quartz crystal.

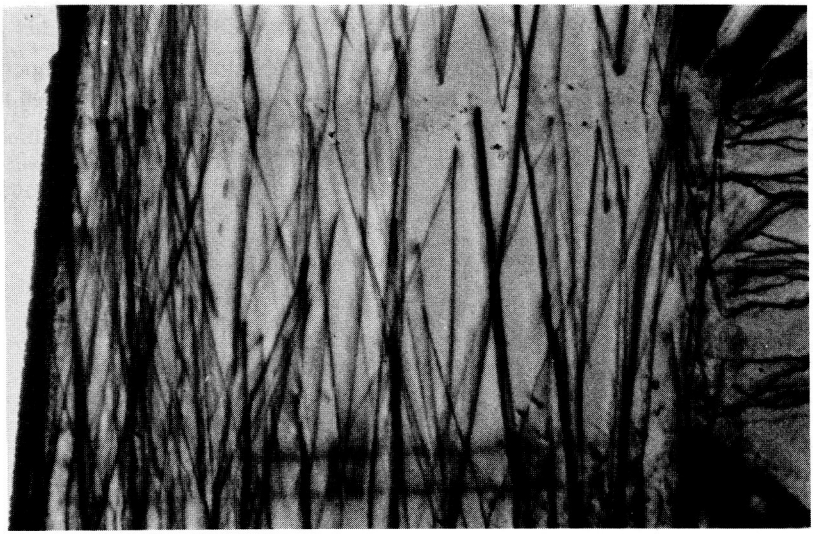

Figure 3. Homogenization temperature of fluid inclusions in the 2A10 sample before experiment. The distribution indicates a filling coefficient of 0.8 which is consistent with the growing conditions for the quartz crystal.

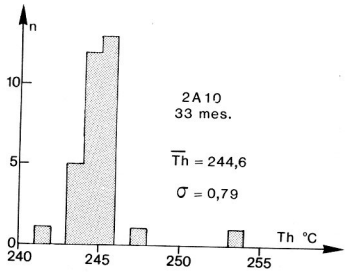

Figure 4. Pressure and temperature diagram showing the (P,T) experimental conditions and the isochore corresponding to the (P,T) hydrothermal growing conditions and to the initial Th of the fluid inclusions. The pressure difference (P_i-P_c) is deduced from the experimental conditions and the isochore position.

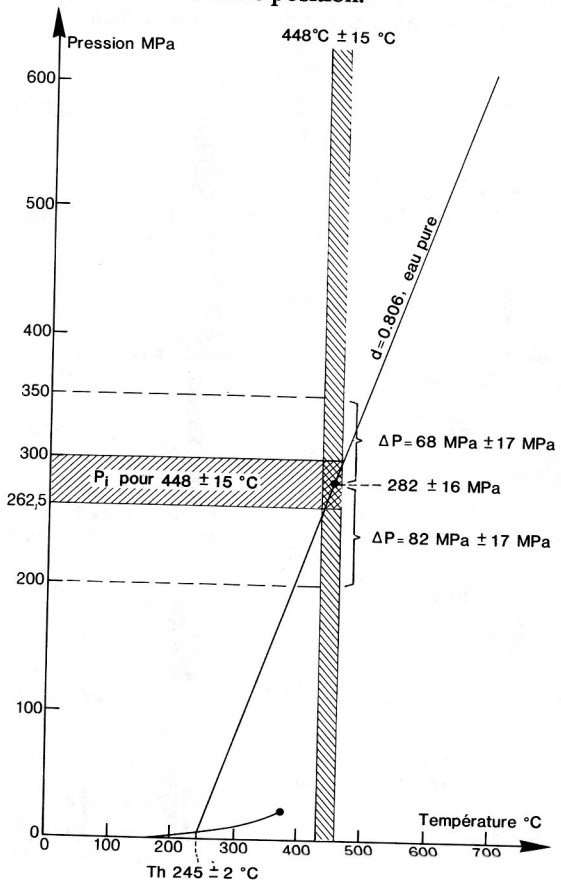

Figure 5. Evolution in time of the shape ratio of the fluid inclusions for both types of experiment. An equilibrium ratio of 2.7 ($P_i > P_c$, losanges) or 1.8 ($P_i < P_c$, squares) is reached after 350h of annealing. The filled symbols correspond to experiments under water confining pressure.

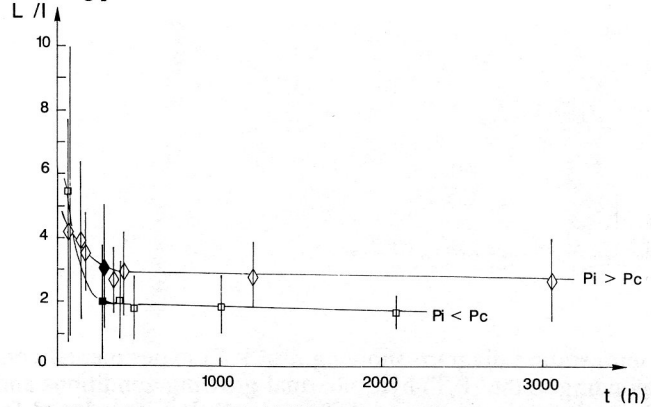

Figure 6. Experiments at T=448°C and P_c=200MPa. Histograms of homogenization temperatures of fluid inclusions after experiments. The hatched band represents initial Th; the star corresponds to experiment with water as the confining medium

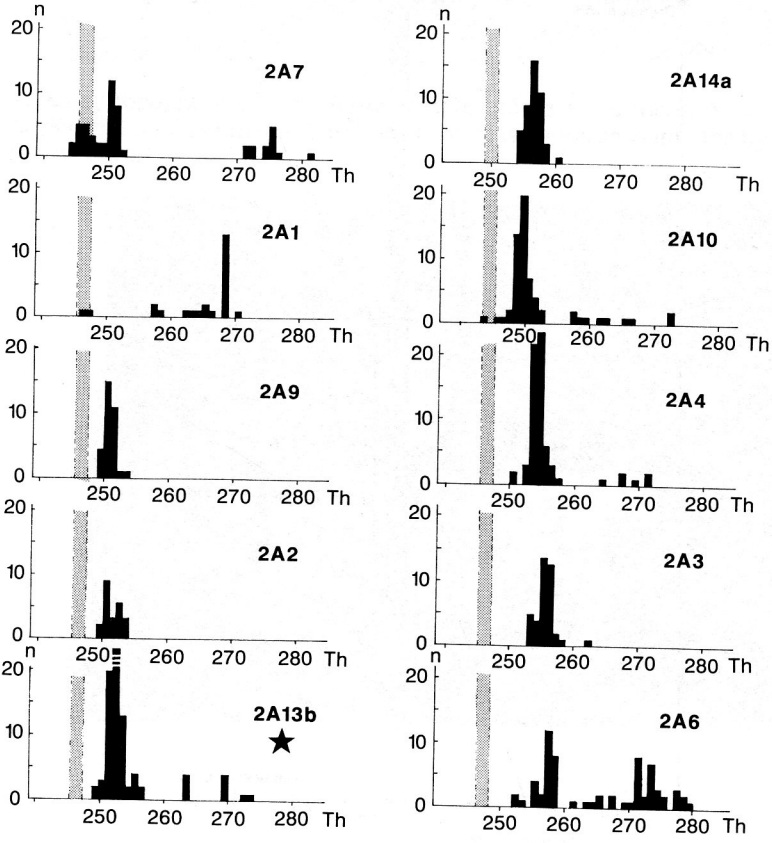

Figure 7. Th variations versus duration of experiments in the case where $P_i<P_c$.

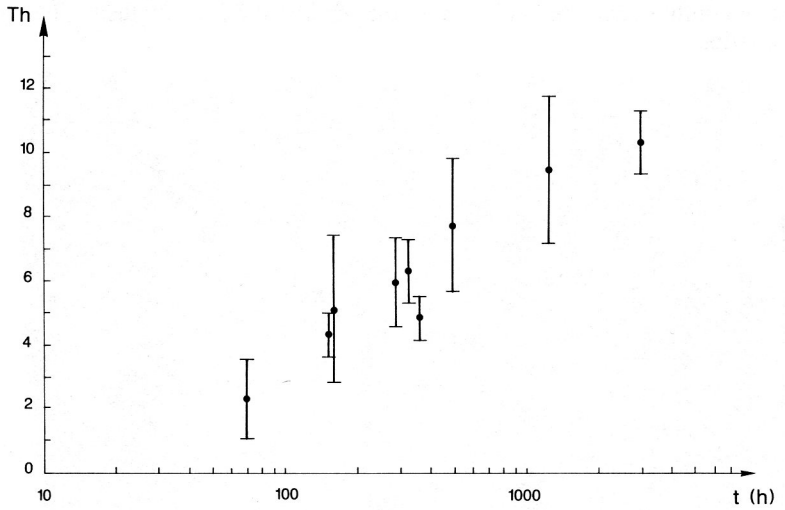

Figure 8. Experiments at T=448°C and P_c=350MPa. Histogramms of homogenization temperatures of inclusions after experiments. The hatched band represents initial Th; the star corresponds to experiment with water as the confining medium.

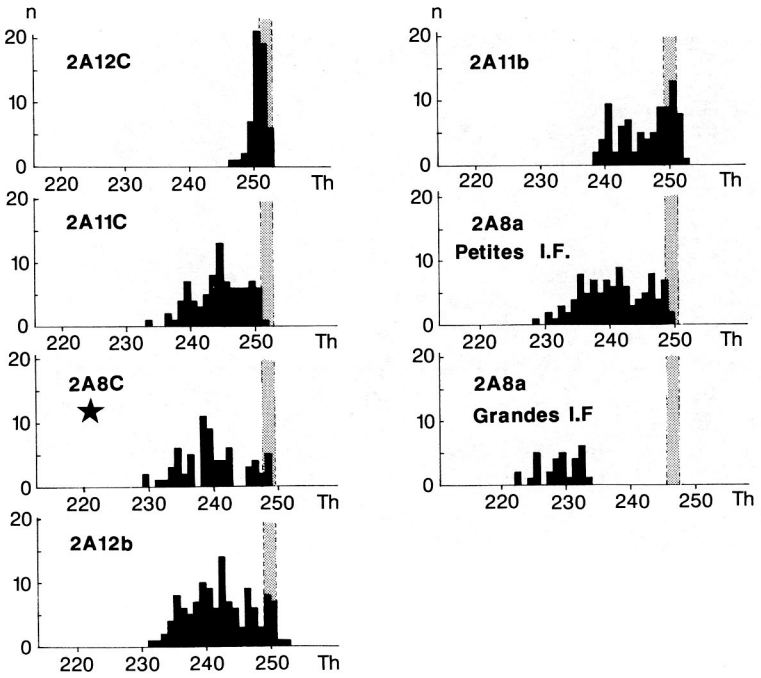

Figure 9. Variations of Th versus $L.l^2$ (proportional to the inclusion volume for initial cylindrical inclusions) for the 2A8c sample ($P_i<P_c$, t=281h 55mn). This diagram does not represent an equilibrium state but indicates that greater the fluid inclusion, larger (or faster) the Th variation.

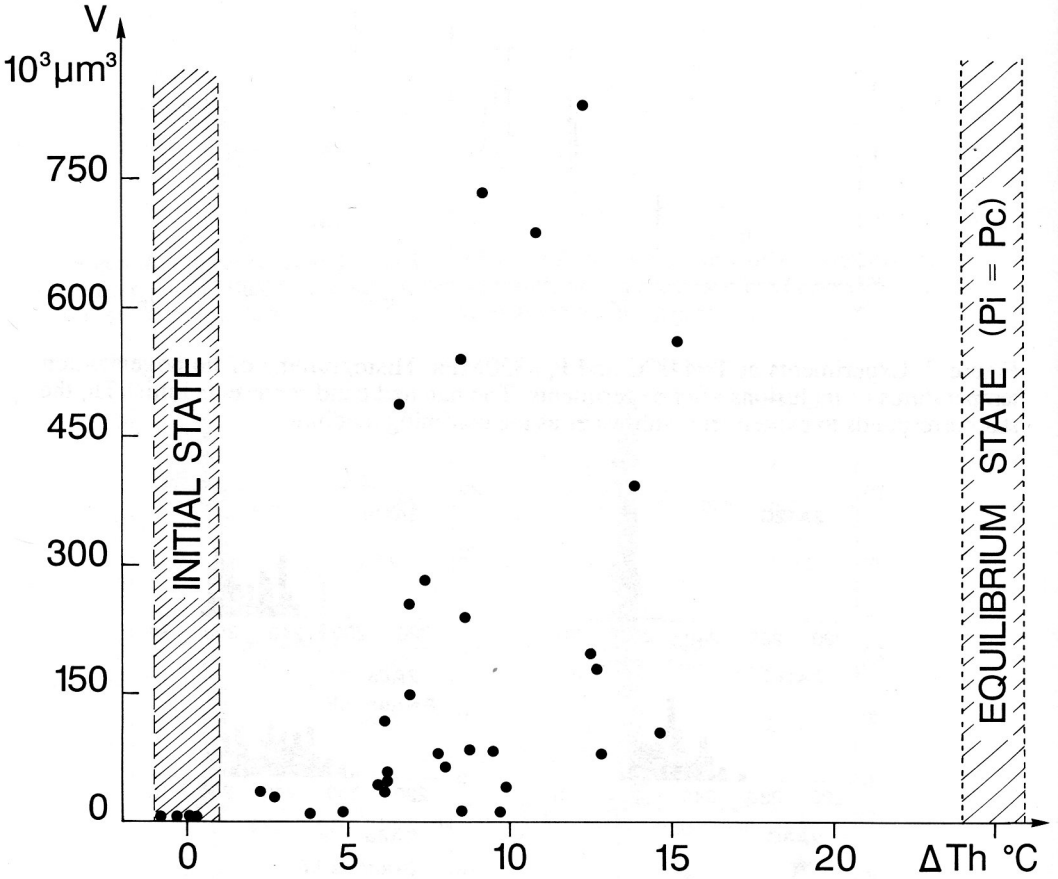

Figure 10. X-ray topographs in a Lang chamber for samples after experiments. a) 2A14a sample, (10$\bar{1}$1) reflexion (P_c=200MPa, T=448°C). Compare this topograph with the figure 2 (same sample before experiment). b) 2A8a sample, (10$\bar{1}\bar{1}$) reflexion (P_c=350MPa, T=448°C).

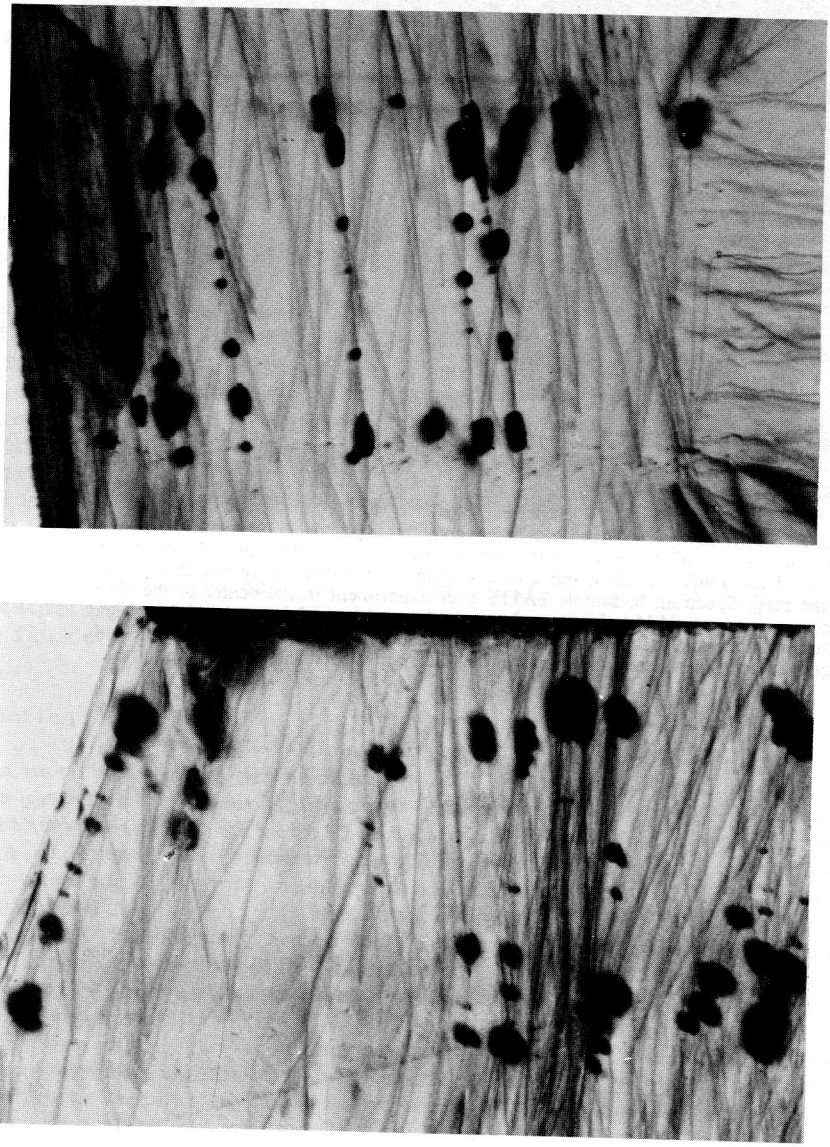

Figure 11. Microphotograph on transmission electron microscope showing dislocations near a fluid inclusion in the 2A4a sample after experiment. The dislocation density is about $10^7 cm^{-2}$.

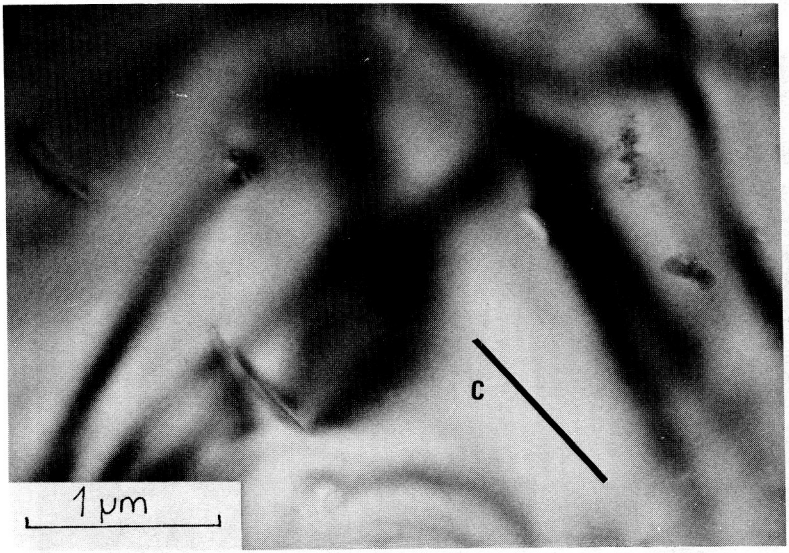

Figure 12. Infra-red spectra in samples before and after experiments. A sketch represents a schematic section of the seed with the two families of fluid inclusions. The beam was focalized near a fluid inclusion. Spectrum a: sample 2A11 before experiment, in the center of the seed. Spectrum b: sample 2A11b after experiment in the center of the seed. Spectrum c: sample 2A11 before experiment in the extremity of the seed with large fluid inclusions. Spectrum d: sample 2A8a after experiment in the extremity of the sample with large fluid inclusions. Scale is identical for the four spectra but a and b have been shifted.